A TUTORIAL ON RETROREFLECTORS AND ARRAYS FOR SLR

John J. Degnan, Sigma Space Corporation, 5600 Forbes Blvd. Lanham, MD 20706 USA
John.degnan@sigmaspace.com

A retroreflector or "cube corner" has the property that it reflects incoming light back onto itself . Three types of retroreflectors are, in order of their frequency of use to date: (1) Aluminum back-coated solid; (2) uncoated solid (Total internal Reflection or TIR); and (3) Hollow cube corners. Their advantages and disadvantages are summarized in Table 1.

Type	Al Back-Coated Solid	Uncoated Solid (TIR)	Hollow
Frequency of Use	Most Common	Occasional Use	Not currently used in the visible
Satellite Examples	Most satellites	Apollo, LAGEOS, AJISAI, ETS-VIII	ADEOS RIS, REM, TES
Reflectivity	0.78	0.93	Can approach 1.0
Polarization Sensitive	No	Yes	No – metal coating Yes-dielectric coating
Weight	Heavy	Heavy	Light
Far Field Pattern	Wide	Wide	Narrow
Issues	Metal coatings absorb sunlight and create thermal gradients. Not as well shielded at high altitudes.	Fewer thermal problems but TIR "leaks" at incidence angles > 17°. Polarization effects can reduce cross-section by factor of 4	Thermal heating and gradient effects on joints

Table 1: Retroreflector Properties.

The peak cross-section of a perfect cube corner is given by

$$\sigma_{cc} = \rho A_{cc}\left(\frac{4\pi}{\Omega}\right) = \rho\left(\frac{4\pi A_{cc}^2}{\lambda^2}\right) = \frac{\pi^3 \rho D^4}{4\lambda^2} \qquad (1)$$

where A_{cc} is the area of the cube face presented to the incoming radiation, λ is the laser wavelength, and D is the diameter of a circular aperture cube corner. In general, the far field diffraction pattern (FFDP) is the 2-dimensional Fourier Transform of the entrance aperture as seen by the incoming plane wave. For a circular aperture at normal incidence, the FFDP is the familiar Airy Pattern given by

$$\sigma(x) = \sigma_{cc}\left[\frac{2J_1(x)}{x}\right]^2 \qquad (2)$$

where $J_1(x)$ is a Bessel function, $x=\pi D\sin\theta/\lambda$, and θ is the off-axis far field angle. The pattern consists of a strong central peak with a half-power point at x = 1.6, a first null at x = 3.8, and angular rings at x = 5 and 8.5 with peak intensities, relative to the central peak, of 0.02 and 0.004 respectively .

For plane waves incident at an angle ϕ relative to the cube normal, the cube aperture appears elliptical to the incoming wave. For solid quartz cubes (n=1.44), the effective cross-section is reduced by 50% for $\phi = 13^o$ and to zero at $\phi = 45^o$. For $\phi > 17^o$, TIR reflection breaks down for certain aspect angles and light (laser and solar) can leak into the mounting assembly, which can heat up and produce thermal gradients that disturb the optical response of the cube/ For hollow cubes, the effective cross-section is reduced

by 50% for $\phi = 9^o$ and to zero at $\phi = 30^o$. The range of accepted incidence angles can also be reduced by recessing the cube into its holder in the array.

The *velocity aberration* effect causes the beam to be deflected by an amount $\alpha = 2v/c$ in the forward direction of the satellite motion where v is the relative velocity between the satellite and station and c is the speed of light. If α is large compared to angular width of the retro FFDP, the reflected beam will not be seen by the SLR station. For LEO satellites , α can take on a range of values between the red (α_{max}) and blue (α_{min}) curves in Figure 1 whereas, for HEO satellites, α has a fixed value between 25 (GNSS) and 20 (GEO) μrad. At lunar distances, α is roughly 4 to 5 μrad if one takes into account Earth rotation. The most efficient array design would concentrate all of the reflected energy in the far field annulus formed by α_{max} and α_{min} with the peak cross-section located at α_{min} where the space loss (R^{-4}) and atmospheric transmission losses are highest.

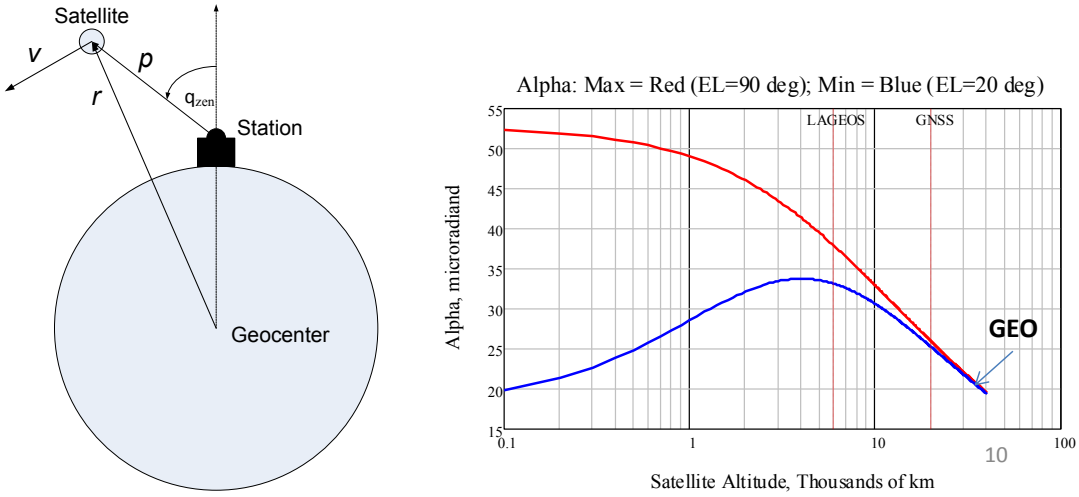

Figure 1: (a) The relative velocity of the satellite seen at the station depends on elevation angle. (b) Maximum velocity occurs at zenith (red curve) while tracking is usually suspended for elevation angles below 20^o (blue curve).

Compensation for velocity aberration is achieved by introducing a *dihedral offset (DO)* between 1 to 3 opposite cube faces. This breaks the central Airy disk into 2N lobes (N=1 to 3). The displacement of the lobes in far field angular space is given by

$$\gamma = \frac{4}{3}\sqrt{6n\delta} \qquad (3)$$

where δ is the dihedral offset from 90^o. Each lobe is the 2D Fourier transform of one 60^o sector of the cube aperture. The large $\Delta\alpha$ for LEOs suggests the use of small diameter cubes to optimally fill the annulus in the radial direction. Gaps in the circumference can then be filled by *clocking* the individual retros in the array; i.e. rotating them within their holders. The small $\Delta\alpha$ for HEOs suggest that larger cubes might be preferred with small step clocking angles to fill in the circumferential gaps.

Flat panel arrays pointed at the Earth CoM from HEO satellites or the lunar surface can have both high cross-section and impulse response. Large radius geodetic satellites with recessed or hollow cubes would provide a narrower impulse response without sacrificing cross-section.

Reference: J.J. Degnan, "Millimeter Accuracy Satellite Laser Ranging: A Review", in Contributions of Space Geodesy to Geodynamics: Technology, D. E. Smith and D. L. Turcotte (Eds.), AGU Geodynamics Series, Volume 25, pp. 133-162, 1993.